



Impact of different land use and land cover in simulation of tropical cyclones over Bay of Bengal

Pushpendra Johari^{1,2} · Sushil Kumar¹ · S. Pattanayak² · A. Routray³ · P. V. S. Raju⁴

Received: 16 March 2023 / Revised: 22 July 2023 / Accepted: 29 July 2023 / Published online: 9 August 2023
© King Abdulaziz University and Springer Nature Switzerland AG 2023

Abstract

This study presents an assessment on the impact of different Land Use/Land Cover datasets in simulating the movement and severity of three extremely severe cyclonic storms, namely Phailin (2013), Hudhud (2014) and Fani (2019), which developed over the Bay of Bengal (BoB). For this purpose, the Advanced Research Weather and Forecasting System (WRF) is selected and the model is forced with necessary input parameters. Two sets of numerical experiment are conducted. The first set of experiments uses U.S. Geological Survey Land Use/Land Cover datasets, and the WRF model is integrated with four different land surface parameterization schemes. The second set of experiments uses the Indian satellite IRS P6 AWiFS-derived Land Use/Land Cover obtained from the National Remote Sensing Centre (here after; AWiFS), and WRF model is integrated with four different land surface parameterization schemes. The model simulated track, mean sea-level pressure, wind, and rainfall are analysed and verified with available observation as obtained from India Meteorological Department and NASA Global Precipitation Measurement. The dynamics and thermodynamic structure are analysed in terms of model simulated vorticity and equivalent potential temperature during the landfall of the system. The results suggested that the use of AWiFS Land Use/Land Cover improves the simulation of track of all the cyclones during and after the landfall of the system. Also, it significantly reduces the landfall point error for all the land surface parameterization schemes except with thermal diffusion scheme. The AWiFS experiments could simulate both the spatial and station rainfall reasonably well. Also, it could simulate the intensity and thermodynamic structure of the cyclone reasonably well.

Keywords Tropical cyclones · Land use/land cover · WRF model · Track · Rainfall · Land surface parameterization schemes

1 Introduction

Indian region is diversified with various land surface features, such as topography, vegetation, soil moisture, soil temperature, soil texture, etc., which are represented by Land

Use/Land Cover (LULC) data. These land surface features impact extreme weather conditions associated with tropical cyclones (TCs). The LULC characteristics have a strong influence in imposing the TCs movement and its severity during and after the landfall of the system. To assess the impact of different LULC in simulating the movement and the severity of landfalling TCs with reasonable accuracy, the forecasting system necessitates an advanced cutting-edge numerical modelling system with precise input parameters. Numerous studies have discussed modelling of cyclone characteristics using the WRF model (Mohanty et al. 2010; Raju et al. 2011; Osuri et al. 2012; Routray et al. 2016; Chauhan et al. 2018; Johari et al. 2022; Tiwari and Kumar 2022). With the advancement of sophisticated data assimilation techniques, such as 3DVar/4DVar and 4DENVar, the predictive skill on tropical cyclones has been improved significantly (Tiwari and Kumar 2023). Several researchers have studied the role of sub-surface and surface properties in

✉ Sushil Kumar
sushil12@gmail.com; sushil.kumar@gbu.ac.in

✉ P. V. S. Raju
pemmani@gmail.com; pvsraju@jpr.amity.edu

¹ Department of Applied Mathematics, USoVSAS, Gautam Buddha University, Greater Noida, India

² RMSI Pvt. Ltd., A-8, Sector 16, Noida, India

³ National Centre for Medium Range Weather Forecasting (NCMRWF), A-50, Sector 62, Noida, India

⁴ Centre for Ocean Atmospheric Science and Technology, Amity University Rajasthan, Kant Kalwar, Jaipur, Rajasthan, India

near-surface meteorology and PBL development (e.g. Betts et al. 1996; Raupach 2000; Maxwell et al. 2007). Alapaty et al. (2008) showed that soil moisture is an important surface parameter that regulates the atmospheric surface energy balance and thus has significant impacts on the vertical distribution of turbulent heat fluxes and the boundary layer structure.

The LULC endures a significant change due to rapid growth and expansion in the emerging anthropogenic diversity and its environmental integration. The land surface process has notable impact on dynamic and thermodynamic exchange process of moisture, momentum and heat (Betts et al. 1996; Anantharaj et al. 2006). These dynamic and thermodynamic changes also affect the atmospheric boundary layer and hence the numerical weather forecasting. Tropical cyclones develop over warm tropical oceans and intensified from the surface water energy. As the cyclone comes closer to the land, LULC has significant role for the movement and intensity of the storm (Gogoi et al. 2019). In tropics, the land use/land cover changes significantly due to colonisation, rapid urbanisation, land degradation, deforestation, landscape fragmentation, etc. (Mohan and Kandya 2015; Singh et al. 2017). Thus, accuracy in LULC information will improve the performance of the numerical weather forecasting models.

Anthes (1984) studied the impact of vegetation surface in increasing the convective precipitation in semiarid region. Collins and Avissar (1994) studied the importance of land surface parameters in atmospheric modelling and suggested that the surface roughness has the major impact. Sateesh et al. (2017) found that the increase of surface drag coefficient in the PBL scheme WRF model leads to the drastic pressure drop and stronger wind in TC simulation. Few studies have been carried out the impact of land surface processes on a climate scale demonstrate strong impact on rainfall (Narisma and Pitman 2003) studied. Pitman et al. (2004) demonstrated the land cover and followed by surface roughness had large impact in simulated rainfall under moisture condition over Australia. Wong and Chan (2006) studied the effect of soil moisture and surface friction on TCs track prediction using MM5 model. The study highlights that the TCs can drift towards land if the roughness length over land is 0.5 m. Also, the soil moisture flux is crucial for TC movement towards land area. Kimball (2009) suggested the sensitivity of surface moisture for precipitation. Many of these studies uses United States Geological Survey (USGS) LULC for the numerical experiments.

The influence of Advanced Wide Field Sensor (AWiFS) LULC data in simulation of track of Severe Cyclonic Storm (SCS) Aila using Mesoscale Model (MM5) was investigated by Badarinath et al (2012). The study also demonstrates the comparison of the performance of USGS LULC and AWiFS LULC for simulation of track and intensity of SCS Aila.

The study suggested that surface roughness and moisture are crucial in predicting the track of cyclone. The study also suggests that the storm position and intensity show a considerable difference between the model integration with AWiFS and USGS data as the system is near to the coast and during the landfall process and moisture content along with surface roughness drives the storm. Srinivasarao Karri et al (2016) made a comparative assessment between AWiFS and USGS LULC on simulation of heavy rainfall and suggested that AWiFS LULC showed more realistic simulation than USGS LULC. The utilisation of AWiFS LULC in WRF model is also highlighted by Ravindranath and Ashrit (2010).

The present study demonstrates the impact of USGS and AWiFS LULC in simulating the movement and severity of Extremely Severe Cyclonic Storms (ESCS) Phailin (2013), Hudhud (2014) and Fani (2019) that formed over the Bay of Bengal (BoB) using Advance Weather Research and Forecasting (WRF) model. A brief description about USGS and AWiFS LULC data is presented in Sect. 2. Section 3 comprises the experimental design and study area followed by the synoptic conditions of Hudhud and Fani in Sect. 4. The results and discussion are presented in Sect. 5 and Sect. 6 highlights the conclusions.

2 Comparison of USGS and AWiFS LULC

The U.S. Geological Survey (USGS) global land cover characterisation LULC dataset (GLCC) was derived from Advanced Very High-Resolution Radiometer (AVHRR) high-resolution (1 km) data considering the period April 1992–March 1993 [Loveland et al. 2000 (modified level 2)]. The USGS data have 24 categories of LULC features and available at 1 degree, 30 min, 10 min, 5 min, 2 min and 30 s resolutions. In India, an effort has been made to develop Indian satellite-based land use and land cover data from IRS-P6, treated as AWiFS datasets. These data are compatible to use in MM5 and WRF models for weather forecasting (Gharai 2014). AWiFS data have four spectral bands with 56 m resolution. The classification of AWiFS data is done with Lambert Conformal projection and World Geodetic System 84-datum.

2.1 USGS and AWiFS LULC Datasets

The USGS LULC data is resulting from MODIS 1 km horizontal resolution data and AWiFS data is created at 56 m spatial resolution from RESOURCESAT of IRS P6. Gharai (2014) also demonstrated on the importance of high-resolution mapping of the satellite product. It is worthwhile to mention that the use of direct measurement (observation) and the classification used in AWiFS data improve the data

accuracy. The USGS data contains 25 LULC categories, whilst AWiFS has 19 categories. Thus, AWiFS data have been reorganised to 25 categories as of the USGS data classes. The ERDAS imagine formatted AWiFS data then converted to Band Interleaved by Pixel (BIP) format for data processing. In case of USGS data, there are 360×180 data points for $1^\circ \times 1^\circ$ resolution, equivalent to 111 km. Similarly, 30 min data have 720×360 data points, equivalent to 55.5 km spatial resolution. The high-resolution 30 s data is nearly equivalent to 1 km. So, in order to generate 30 Second WRF compatible data, 30 s AWiFS regrouped data geo-referenced to form 25 classes as of USGS data. There are 16 such geo-referenced AWiFS data tiles need to be prepared for WRF model integration. The details on the AWiFS datasets can be found from National Remote Sensing Centre (NRSC) of Indian Space Research Organisation (ISRO) (www.nrsc.gov.in) under Bhuvan portal.

The LULC coverage for cyclones Phailin, Hudhud and Fani with USGS and AWiFS data are presented in Fig. 1. The AWiFS data are updated on annual basis (NRSC Tech. Report, 2014) and thus the AWiFS data for 2013–2014 are considered for cyclone Phailin. AWiFS data for 2014–2015 are considered for cyclone Hudhud, and the AWiFS data for 2018–2019 are used for cyclone Fani. The area surrounded by landfall location for each cyclone is marked with maroon-coloured circle. In case of Phailin, the landfall location is Gopalpur, and the area surrounded by it is duly marked in both the LULC data in Fig. 1 (top panel). In case of USGS, the marked area is covered with grassland/shrubland/cropland, and with AWiFS data, it is covered with water bodies/evergreen broadleaf forest/irrigated cropland/dryland. A sharp contrast is noticed in AWiFS data. In case of Hudhud, the landfall location is Visakhapatnam and the area surrounded by it is marked in both the datasets in Fig. 1 (middle panel). In case of USGS data, this area is covered with cropland/irrigated cropland/mixed dryland, whilst the AWiFS data classified the same area with water bodies/evergreen broadleaf forest/urban and build-up land pasture. This suggests that there is sharp contrast in the surface roughness and moisture potential between AWiFS and USGS LULC data in the marked area. Similarly, the Fani cyclone made landfall on Puri and the surrounding area is marked with maroon-coloured circle in both the datasets as shown in Fig. 1 (bottom panel). In case of USGS, the majority of the area is covered with mixed dryland, whereas AWiFS data classified it as dryland/urban build-up/grassland, etc. Again, there is a significant variation in surface roughness between AWiFS and USGS datasets in the marked area.

The above comparison of USGS and AWiFS LULC datasets for 2013, 2014 and 2019 clearly shows that AWiFS has high spatial resolution for the category detection and classification for the cyclones of interest. It may further be noted that NRSC-generated LULC classifications over

the Indian continent in regional domain were finalised in detailed discussions within the Central/State government departments/institutions (NRSC 2014), whilst USGS is a global data classified for global use. Hence, AWiFS LULC data are more representative of ground conditions. Thus, it has been hypothesised that the incorporation of AWiFS land use coverage will improve the simulation of track and severity of ESCSs Phailin, Hudhud and Fani, especially during landfall process.

3 Experimental Design and Study Area

Based on the previous study on tropical cyclone simulations, we have adopted Kain Fritsch cumulus scheme, Ferrier microphysics and YSU planetary boundary layer scheme (Raju et al. 2011; Osuri et al. 2012; Shenoy et al. 2022). In the present study, four land surface parameterization schemes are used in the WRF model to simulate the movement and severity of Phailin, Hudhud and Fani cyclones (Table 1).

Two sets of numerical experiment—(1) with USGS LULC and (2) with AWiFS LULC are conducted for both cyclones and with each set of experiment having four sub-experiments, one for each land surface parameterization scheme. Hence, a total of eight numerical experiments are carried out for each cyclone using USGS and AWiFS LULC data, and the same are tabulated below in Table 2

In order to perform the above-mentioned experiments, the WRF model is configured with horizontal grid resolution of 9 km with 280×210 grid points. The model is initialised with Final Analysis (FNL) $1^\circ \times 1^\circ$ (latitude–longitude grid) data sets of National Centers for Environmental Prediction (NCEP). The data is available in every 6-h interval at <https://rda.ucar.edu/datasets/ds083.2/>. Each LULC dataset used in this analysis has 30 s horizontal resolution. The USGS LULC datasets are downloaded from website https://www2.mmm.ucar.edu/wrf/users/download/get_sources_wps_geog.html. The AWiFS datasets are obtained from National Remote Sensing Centres (NRSC), Hyderabad. The observed storm location and severity of the system are taken from the India Meteorological Department (IMD) published report for respective.

4 Results and Discussion

The influence of the USGS and AWiFS LULC in simulation of key characteristics of the TCs Phailin, Hudhud and Fani is analysed and highlighted in results and discussion. The model simulated track is verified with the best-fit observed track of India Meteorological Department (IMD). The model simulated mean sea-level pressure (MSLP) and maximum sustainable wind (MSW) are also analysed and presented.

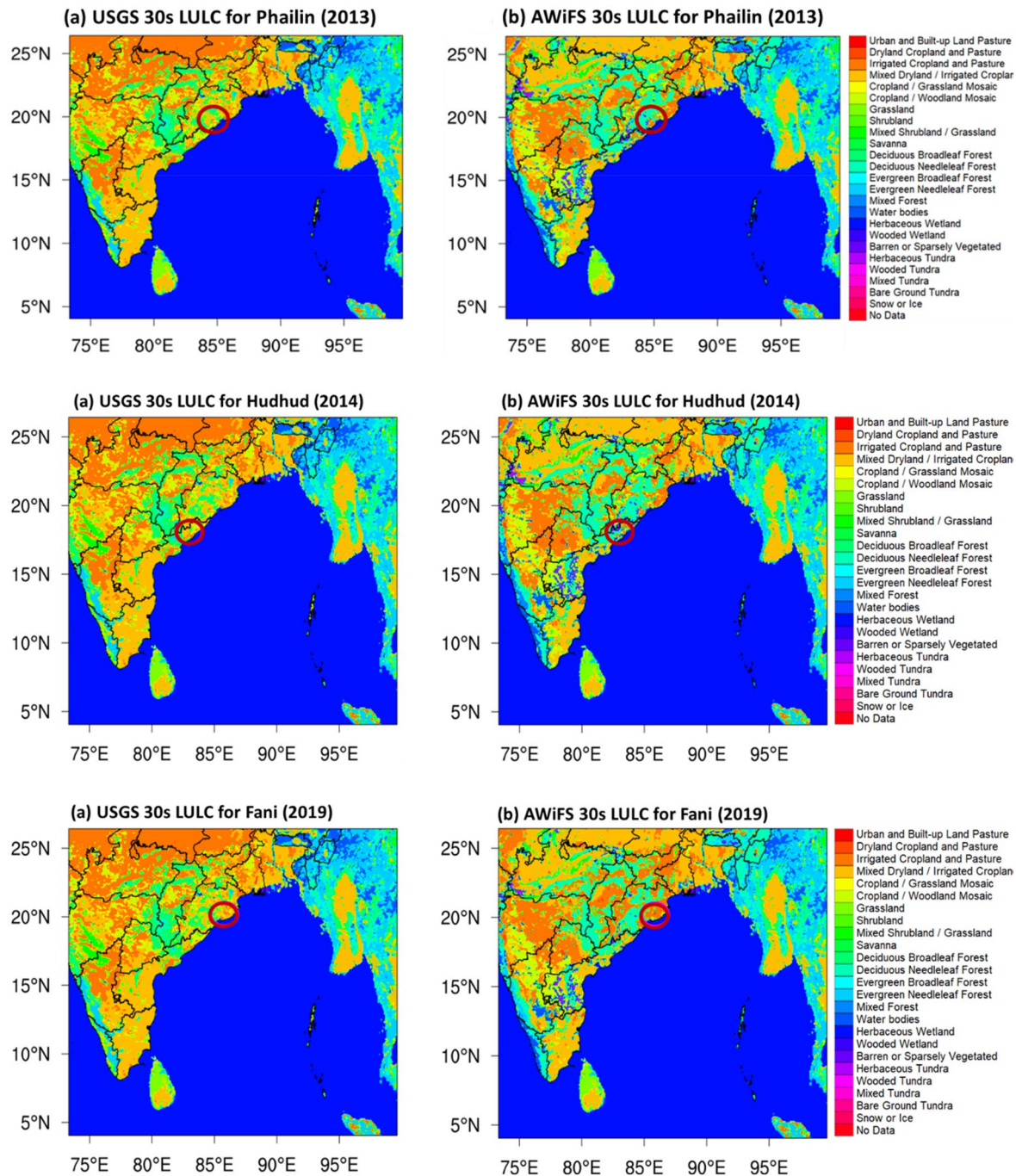


Fig. 1 LULC coverage for cyclone Phailin, Hudhud and Fani with **a** USGS and **b** AWiFS data

Model simulated spatial rainfall is verified and compared with the Global Precipitation Measurement (GPM) gridded rainfall. The location-specific simulated rainfall (stations near the landfall location of the system) is also compared with two different data sources like GPM and IMD observed rainfall on particular stations. Along with this, a few diagnostic parameters, such as vorticity and equivalent potential temperature, are also estimated from the model

simulation to showcase the thermodynamics structure of the cyclones.

4.1 Simulation of Cyclones Tracks

The simulation track of three cyclone was initialised with NCEP-FNL data with USGS and AWiFS LULC, respectively depicted in Fig. 2. The track of the cyclone Phailin has

Table 1 Synoptic overview of Phailin, Hudhud and Fani cyclones

S. No	Cyclone name	Landfall place and time	Duration of the system	Salient features
1	Phailin (ESCS)	Landfall Location: Gopalpur, coast of Odisha Landfall Time: 2230 h IST of 12th Oct. 2013	08–14 October, 2013	1. The most intense, rapid intensified cyclone that crossed the coast of Odisha after the Super Cyclone 1999 Very heavy to extremely heavy rainfall over Odisha leading to floods, and strong gale wind leading to large-scale structural damage and storm surge leading to coastal inundation over Odisha
1	Hudhud (ESCS)	Landfall location: Visakhapatnam, coast of Andhra Pradesh Landfall Time: 1200–1300 IST, 12th October 2014	07–14 October, 2014	Cyclone which crossed Visakhapatnam, the coast of Andhra Pradesh in October after a huge gap of nearly 30 years. Strong wind and extreme rainfall caused a huge damage in north Andhra Pradesh and South Odisha regions
2	Fani (ESCS)	Landfall Location: Puri, coast of Odisha Landfall Time: 0800–1000 IST, 3rd May 2019	26 April 2019–04 May 2019	The system originated near the equator $\sim 2.7^\circ$ latitude, which is very rare in the development of tropical cyclones Most intense storm for the Odisha coast during pre-monsoon season in a climate scale The storm covers a recorded length of 3030 km, which is very unique for BoB system

Table 2 Experimental design used in the present study

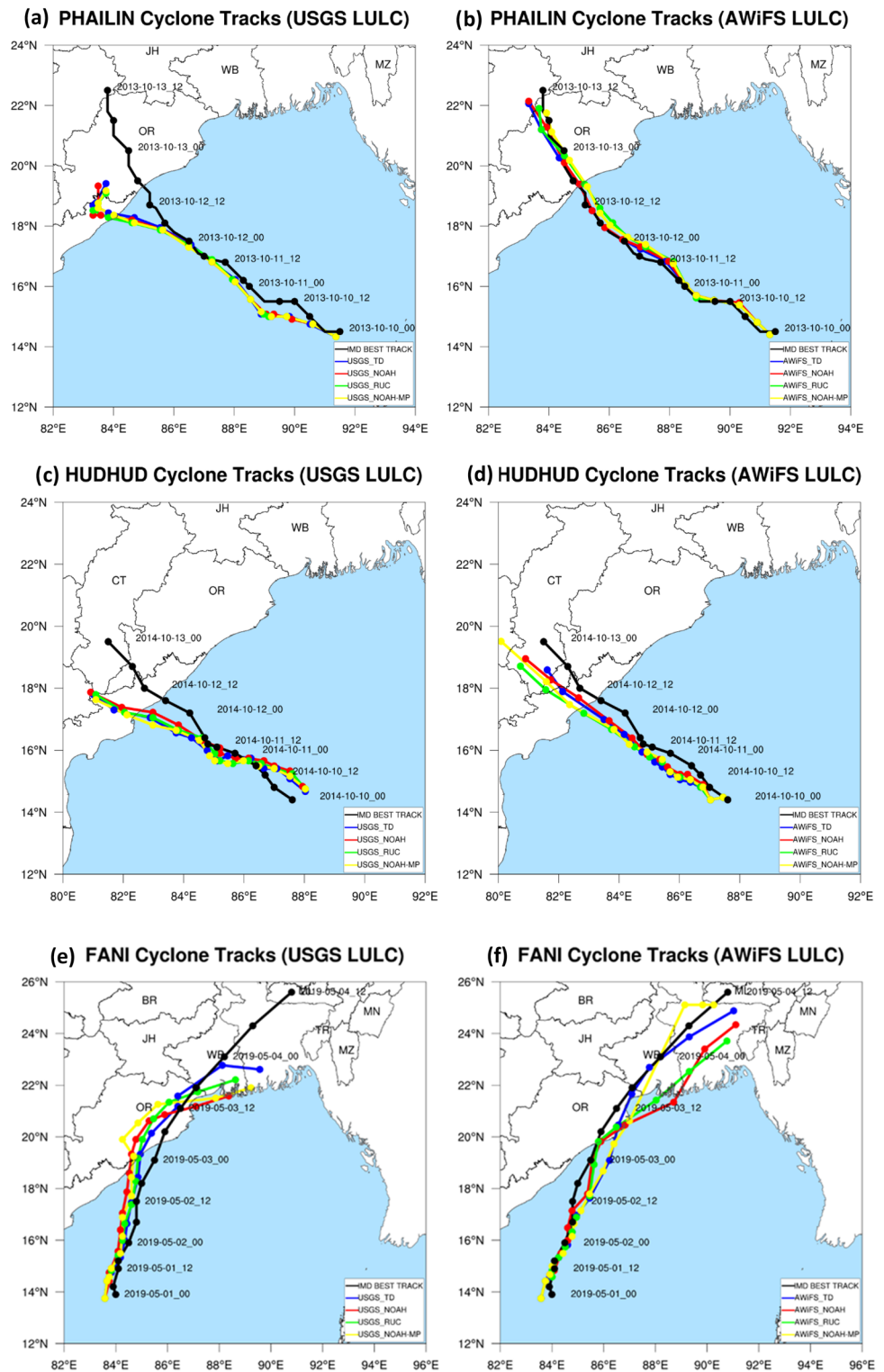
Sl. No	LULC data	Land surface processes	Physics common to all experiments
1	USGS	Thermal Diffusion	Cumulus: Kain Fritsch scheme
2		NOAH	
3		RUC	
4		NOAH-MP	
5	AWiFS	Thermal Diffusion	PBL: YSU scheme
6		NOAH	
7		RUC	
8		NOAH-MP	
			Surface Layer Parameterization: Monin Obukhov scheme Radiation: RRTM (Long-wave)/Dudhia (Short-wave)

shown that there is a large deviation in the model simulated landfall position with USGS LULC (Fig. 2a). The simulated track moved in westward direction just before the landfall of the system. However, the experiments with AWiFS LULC significantly improve the track prediction with a very minimal landfall point error (Fig. 2b). The details about the landfall position and time error are provided in Table 3.

In case of Hudhud, the model is initialised with NCEP-FNL data at 00 UTC of 10 October 2014. Figure 2c represents WRF model simulated tracks with four diverse land surface parameterization processes as stated above and using USGS LULC along with the observed track of IMD for the ESCS Hudhud (IMD report 2014). Figure 2d presents WRF model simulated tracks with four land surface parameterization processes and using AWiFS LULC. The model simulated tracks with USGS LULC (Fig. 2c) move

in west–north–westward direction, going away from the observed track of the cyclone, whereas AWiFS simulated tracks (Fig. 2d) first move in westward direction and then drifted towards north–westward direction, coming closer to the observed track of the cyclone during and after the landfall of the system. This northward drift with AWiFS datasets is mainly attributed to the larger roughness contrast in land and sea for the area of interest than in USGS datasets. The landfall point and time error are also estimated WRT the observed storm location and time. It may be seen that all the land surface schemes except “Thermal Diffusion” provide less landfall point error in AWiFS experiments than in USGS experiments. The NOAH-MP scheme depicts comparatively less error than any other schemes for both USGS and AWiFS LULC. However, the use of AWiFS data sets significantly reduces the landfall errors. It is also noticed that both the

Fig. 2 Model simulated cyclone track with two LULC data of **a** Phailin-USGS, **b** Phailin-AWiFS, **c** Hudhud-USGS, **d** Hudhud-AWiFS, **e** Fani-USGS, **f** Fani-AWiFS



sets of experiments are showing delay in landfall time of the system than the actual landfall of the system. The details on the landfall location and time error are provided in Table 4.

In case of ESCS Fani, the WRF model is initialised at 00 UTC 01 May 2019. Figure 2e and f represents the model

simulated tracks with four land surface parameterization schemes using USGS and AWiFS LULC, respectively, along with the IMD observed track (IMD report 2019). It is noticed that the track of the cyclone from model simulation initially moved northward and then north-eastward direction, similar

to the observed track. The model simulated tracks using USGS LULC are moving to the left of the observed track throughout the lifecycle, showing increase in track error and separated a distant away from the IMD best-fit track. However, the model simulated tracks with AWiFS LULC are to the right of the IMD observed track and nearly coinciding with IMD track, resulting less track error during landfall time. Furthermore, it is seen that the model simulated track using AWiFS LULC and NOAH-MP parameterization scheme is performing better as compared to other schemes during the landfall process, whilst the model simulated track is far from the observed track for USGS LULC. Table 5 shows the model simulated landfall point and time error calculated with respect to IMD observations for four

parameterization schemes. The analysis clearly suggests that all the land surface schemes except “Thermal Diffusion” are providing less landfall point error in AWiFS LULC experiments than that of the USGS LULC. The landfall time error is also significantly reduced with the use of AWiFS LULC as compared to USGS LULC.

The overall analysis on the simulation of track of the cyclones clearly suggests that the inclusion of realistic representation of the land surface features, surface roughness, moisture potential and more specifically the roughness contrast between land and sea plays an important role in numerical modelling. Experiments also show that the use of NOAH-MP land surface parameterization scheme performing better in simulating the track and consequently

Table 3 WRF model simulated landfall location and landfall time error for TC Phailin

Experiment no (Land Surface Schemes)	WRF model simulation			
	USGS LULC		AWiFS LULC	
	Landfall point error (km)	Landfall time error (h)	Landfall point error (km)	Landfall time error (h)
Expt—1 (TD)	156.6	− 0.5	5.4	+0.5
Expt—2 (NOAH)	169.8	− 5	6.2	+0.5
Expt—3 (RUC)	180.4	− 2	6.8	+0.5
Expt—4 (NOAH-MP)	155.9	− 2	6.0	+0.5

± sign in landfall time indicates the delay/early landfall of the system

Table 4 WRF model simulated landfall location and landfall time error for TC Hudhud

Experiment no (Land Surface Schemes)	WRF model simulation			
	USGS LULC		AWiFS LULC	
	Landfall location error (km)	Landfall time error (h)	Landfall location error (km)	Landfall time error (h)
Expt—1 (TD)	161.7	+ 10	295.4	+9
Expt—2 (NOAH)	144.6	+9	78.5	+8
Expt—3 (RUC)	146.8	+9	137.1	+8
Expt—4 (NOAH-MP)	133.4	+9	63.1	+8

± sign in landfall time indicates the delay/early landfall of the system

Table 5 WRF model simulated landfall location and time error for Fani

Experiment no (Land Surface Schemes)	WRF model simulation			
	USGS LULC		AWiFS LULC	
	Landfall location error (km)	Landfall time error (h)	Landfall location error (km)	Landfall time error (h)
Expt – 1 (TD)	129.6	+ 11.3	175.4	− 1.5
Expt – 2 (NOAH)	128.5	+ 16.5	7.8	+1
Expt – 3 (RUC)	122.0	+ 8.5	36.9	+3
Expt – 4 (NOAH-MP)	131.9	+ 5.5	6.4	− 0.5

± sign in landfall time indicates the delay/early landfall of the system

reduces the landfall point and time error significantly over BoB region.

4.2 Mean Sea-Level Pressure and Maximum Wind

The mean sea-level pressure (MSLP) and maximum sustained wind (MSW) are also estimated from model simulation and compared with the IMD estimated value for the ESCSs Phailin, Hudhud and Fani and presented in this section. The analysis on model simulated MSLP clearly shows that the experiments with USGS data overestimate the MSLP value for all the parameterization schemes. However, the results improved with AWiFS experiments. Results suggest that the RUC parameterization scheme is rapidly intensifying the storm. The observed maximum MSLP was 940 hPa and the experiments with USGS could simulate up to 910 hPa with RUC scheme and it is 938 hPa with AWiFS data. The intensification and the dissipation of the storm are well presented by the model simulation though there is an early intensification is noticed. Similarly, the model simulated MSW (kmph) is estimated and compared with IMD observed value. The observed maximum wind was

212 kmph and the model could simulate 260 kmph with USGS experiment and RUC scheme, and it is 227 kmph with AWiFS experiment. The details of the MSLP and MSW during the landfall of the storm are projected in Table 6. Hence, it is worthwhile to mention that the WRF model with RUC land surface parameterization scheme and AWiFS LULC could well simulate the maximum wind during the landfall time.

The IMD observed and WRF model simulated MSLP and MSW during the landfall for the cyclone Hudhud are presented in Table 7. It is noticed that the observed minimum MSLP was 950 hPa at 06 UTC 12 October 2014, and the experiment with RUC land surface parameterization scheme and NRSC LULC data could simulate 945 hPa with a delay of 6 h i.e. at 00 UTC 13 October 2014. The use of USGS LULC further intensifies the storm to 932 hPa at 00 UTC 13 October 2014.

It is seen that during the landfall of the system, the observed maximum wind is 185 kmph, and the model could simulate up to 172 kmph with NOAH-MP parameterization scheme. The experiments with AWiFS LULC further intensify the storm to 180 kmph with a delay of 6 h i.e. at

Table 6 Observed and WRF model simulated MSLP and MSW for TC Phailin

LSP schemes	LULC	MSLP (hPa) at landfall time (1800 UTC/12th October)		Wind Speed (kmph) at landfall time (1800 UTC/12th October)	
		Observed (IMD)	WRF model simulated	Observed (IMD)	WRF model simulated
TD	USGS	956	936.7	185	149
NOAH			938.2		148
RUC			924.3		227
NOAH-MP			940.2		149
TD	AWiFS		950.4		149
NOAH			955.7		144
RUC			954.4		193
NOAH-MP			959.9		139

Table 7 Observed and WRF model simulated MSLP and MSW for TC Hudhud

LSP Schemes	LULC	MSLP (hPa) at landfall time (0600 UTC/12th October)		Wind Speed (kmph) at landfall time (0600 UTC/12th October)	
		Observed (IMD)	WRF model simulated	Observed (IMD)	WRF model simulated
TD	USGS	950	977.7	185	73.0
NOAH			976.6		165.7
RUC			973.5		170.7
NOAH-MP			976.0		172.8
TD	AWiFS		966.8		127.3
NOAH			970.0		165.6
RUC			963.7		164.7
NOAH-MP			972.0		172.8

0000 UTC 13 October 2014. Similarly, the IMD observed and WRF model simulated MSLP and MSW for the cyclone Fani are estimated during the landfall of the system and presented in Table 8.

It is seen that the observed minimum MSLP was 934 hPa at 1800UTC 02 May 2019, and the model could simulate up to 958 hPa. It may be noted that there is not much difference noticed in USGS and NRSC LULC data for different land surface parameterization schemes. The observed and model simulated MSW (kmph) with different land surface parameterization schemes for cyclone Fani are evaluated. It is seen that the observed maximum wind was 213 kmph, and the model could simulate about 210 kmph with RUC land surface parameterization scheme with NRSC land use data sets. It is also noticed that RUC scheme is performing better than any other schemes for USGS LULC as well.

4.3 Simulation of rainfall

The WRF-simulated 24-hour accumulated rainfall is analysed, verified and related with NASA's Global Precipitation Measurement (GPM), available at 10 km horizontal resolution.

Figure 3 represents the spatial distribution of rainfall for cyclone Phailin on the storm's landfall day, October 12 2013. The USGS experiments overestimate the rainfall amount and the maximum rainfall is over ocean. During the landfall of the storm, the rainfall distribution is much towards south of the actual rainfall. However, the AWiFS experiments reasonably well simulated the amount of rainfall. The model simulated daily accumulated rainfall over the landfall location Gopalpur during 11–13 October 2013, which is compared with IMD and GPM rainfall as shown in Fig. 4. The analysis clearly indicates that rainfall amount with AWiFS LULC and NOAH-MP parameterization scheme is well comparable with IMD observation.

Figure 5 depicts the spatial distribution of rainfall for cyclone Hudhud on the storm's landfall day, October 12,

2014. It is noticed that the model simulation with USGS and AWiFS LULC overestimates the rainfall amount than that of the GPM observed rainfall, with the maximum rainfall occurring over the ocean itself. The AWiFS experiments could well simulate the rainfall over the landfall location, Visakhapatnam. Although the AWiFS LULC slightly overestimates the rainfall amount, it could very well represent the amount of rainfall over the landfall region, Visakhapatnam. The model simulated daily accumulated rainfall over the landfall location Visakhapatnam during 10–12 October 2014 clearly indicates that rainfall amount with AWiFS LULC and NOAH-MP parameterization scheme is well comparable with IMD observation (Fig. 6).

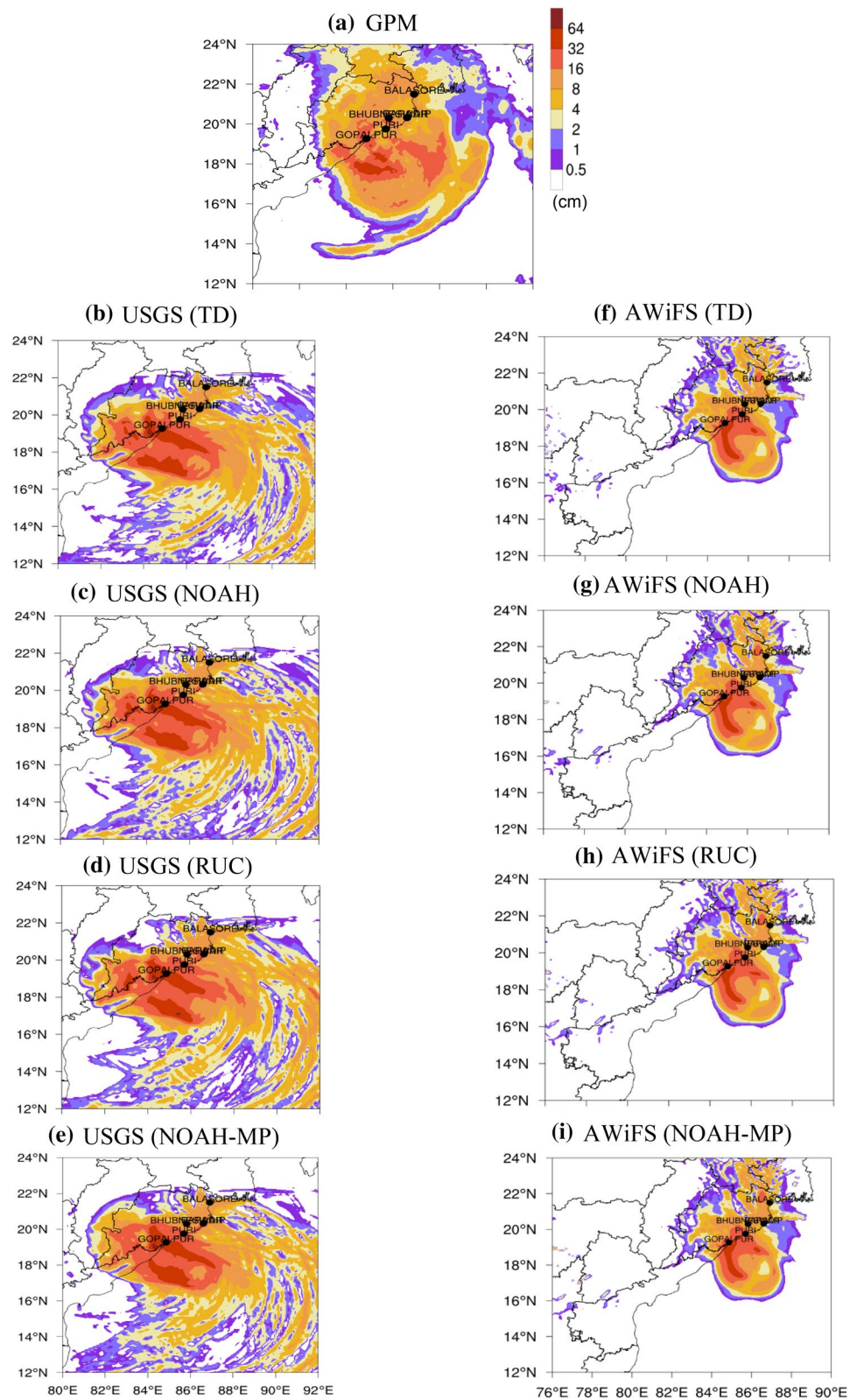
The spatial representation of rainfall for Fani on the storm's landfall day, May 03, 2019 is depicted in Fig. 7. It is seen that the model simulation with USGS LULC overestimates the rainfall amount, but the maximum rainfall is far away from the landfall location. Overall, both the experiments provide more or less in a similar distribution, but there is a north–westward shift in USGS experiment. The model simulated rainfall with AWiFS LULC though slightly overestimates over the ocean. However, it could well be presented over the land region. The model simulated daily accumulated rainfall over the landfall location Puri during 01–03 May 2019 is compared with IMD and GPM rainfall as shown in Fig. 8. The analysis clearly indicates that rainfall amount with AWiFS LULC and NOAH-MP parameterization scheme is in good agreement with IMD observation.

Overall, the model simulated rainfall indicated that experiment with AWiFS LULC well captured the rainfall amount. The USGS experiments underestimated the rainfall amount on 02 May 2019, whilst the simulated rainfall amount improved on 03 May 2019. The AWiFS experiments overestimated the rainfall amount on 03 May 2023. Overall, the NOAH-MP parameterization scheme accurately presented the rainfall amount and provided a reasonable comparison with the IMD rainfall over Puri.

Table 8 Observed and WRF model simulated MSLP and MSW for TC Fani

LSP Schemes	LULC	MSLP (hPa) at landfall (0300 UTC/3rd May 2019)		Wind Speed (kmph) at landfall (0300 UTC/3rd May 2019)	
		Observed (IMD)	WRF model simulated	Observed (IMD)	WRF model simulated
TD	USGS	950	965.2	185	73.0
			961.6		165.7
			962.8		170.7
			963.3		172.8
TD	AWiFS		959.2		127.3
			959.0		165.6
			958.9		164.7
			958.3		172.8

Fig. 3 24-h accumulated rainfall (cm) associated with Phailin from **a** GPM, **b–e** USGS LULC, and **f–i** AWiFS LULC on the landfall day, 12 October 2013

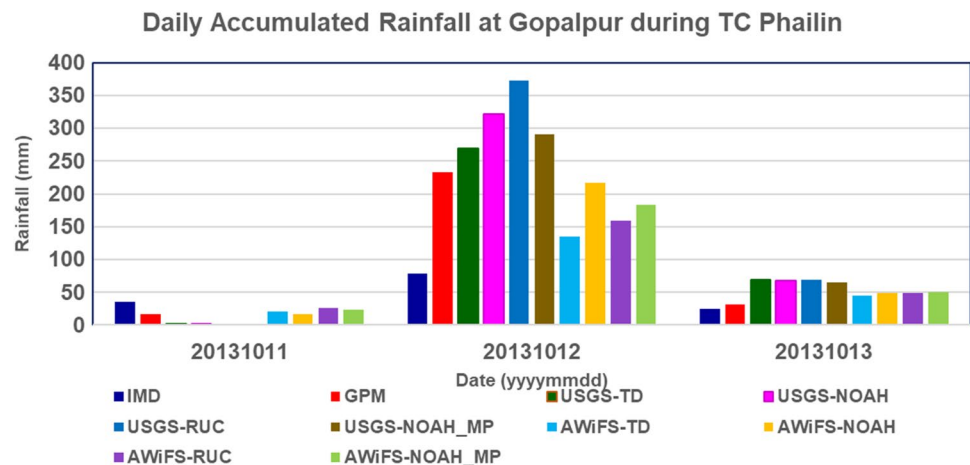


4.4 Structure of TC

The initiation, development, movement, structure and intensity of tropical cyclones embedded in multi-scale

interactions of associated weather phenomenon. The dynamic framework related to the TC structure and motion greatly depends on the positive potential vorticity anomaly from the environmental flow and in the same way, the

Fig. 4 Comparison of WRF-simulated daily accumulated rainfall associated with TC Phailin with IMD and GPM observation over Gopalpur during 11–13 October, 2013



intensity of low-level equivalent potential temperature quantifies the total thermodynamic energy associated with tropical cyclone. Several studies (Wu and Emanuel 1993; Wu and Kurihara 1996; Wang et al 1998) directed that the motion is mostly influenced by the steering flow associated with the large-scale environment, whereas the inner core structure and its severity explicitly were impacted by the close interaction of complex physical processes and also associated with the ocean–atmosphere energy exchange processes (Wu and Cheng 1999; Bosart et al 2000; Hong et al 2000; Wang 2002). Hence, the understanding and the numerical forecasting of cyclone structure and its changing severity are difficult tasks than forecasting the movement of cyclone. The vorticity and equivalent potential temperature are presented for cyclone Phailin at the landfall day. Figure 9 demonstrates the spatial distribution of WRF model simulated vorticity at 850 hPa for TC Phailin from both USGS and AWiFS LULC valid on 12 October 2013. It is noticed that the model simulation with USGS LULC has a wide horizontal extension with higher intensity than the AWiFS experiment. However, the location of the maximum vorticity is much south to the actual landfall location. In case of AWiFS, the maximum vorticity value is comparatively less, but it is closer to the observed landfall location. The vertical extent of the vorticity field is estimated through latitudinal cross section indicated that both the experiments could capture the vertical extent reasonably well (Fig. 10). However, the value of vorticity about $150 \times 10^{-5} \text{ s}^{-1}$ extended up to 400 hPa in the case AWiFS than the USGS LULC run. It is clearly seen that low vorticity is observed in higher pressure levels which suggested that the strong low-level convergence and upper-level divergence properly ascertain in the AWiFS.

The model simulated equivalent potential temperature is presented in Fig. 11. Both the experiments well simulated the equivalent potential temperature; however, USGS LULC depicts southward shift of the vortex core during the landfall

of the system. Figure 12 represents the vertical cross section of the equivalent potential temperature at the landfall day of TC Phailin. The sharp extension of equivalent potential temperature up to 300 hPa clearly indicates the symmetric structure of the system in lower and middle levels. With the evidence from other observational and modelling studies, the positive vorticity and the equivalent potential temperature with high values is confined to a narrow radius of the system.

5 Conclusions

The present study examines the performance of WRF model in simulation of landfalling tropical cyclones over Bay of Bengal with the use of USGS and AWiFS LULC data. The study also emphasises the performances of various land surface parameterization schemes along with the USGS and AWiFS LULC categories. The model simulated key parameters, such as track, MSLP, MSW, and rainfall, are analysed and compared with observation. The India Meteorological Department best-fit track, MSLP, MSW and station rainfall data are used for verification of the model parameters. Also, the NASA's Global Precipitation Measurement gridded rainfall data are used for spatial verification of rainfall. The dynamics and the thermodynamic structure of the storm are analysed in terms of model simulated vorticity and equivalent potential temperature during the landfall of the system.

The spatial representation of USGS and AWiFS LULC data for the years 2013, 2014 and 2019 in the periphery of landfall location of cyclones considered in this study clearly demonstrates a large variation in both the datasets. The AWiFS data have high spatial resolution for the category detection and classification for the cyclones of interest than that of USGS data. It is worthwhile to mention that AWiFS LULC is generated in considering the classifications over the Indian continent and with

Fig. 5 24-h accumulated rainfall (cm) associated with Hudhud from **a** GPM, **b–e** USGS LULC, and **f–i** AWiFS LULC on the landfall day, 12 October 2014

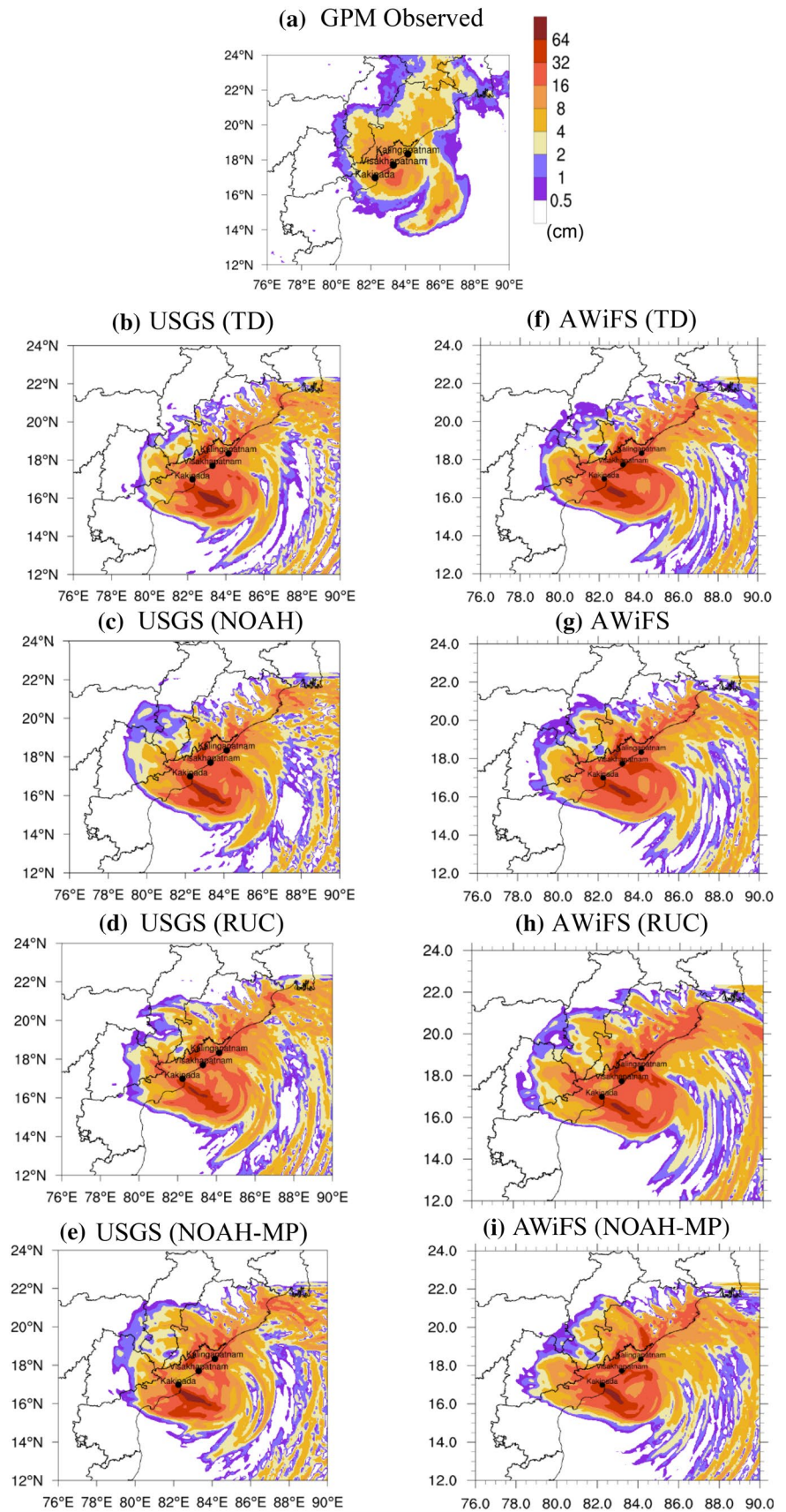
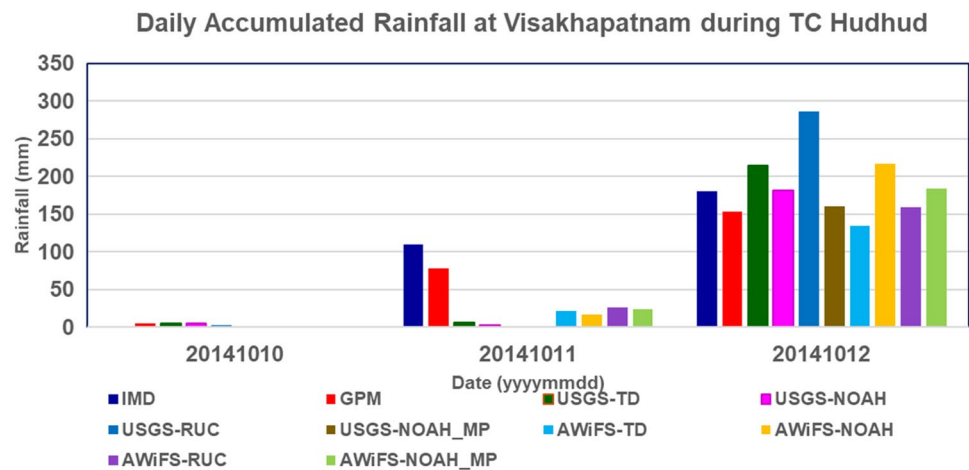


Fig. 6 Comparison of WRF model simulated daily accumulated rainfall associated with TC Hudhud with IMD and GPM observation over Visakhapatnam for 10–12 October, 2014



incorporation of ground truth, whilst the USGS LULC is a global data classified and designed for global use. Hence, AWiFS LULC data are more representative of ground conditions.

The model simulated track improved noticeably with the use of AWiFS LULC than that of the USGS datasets. In case of Phailin, significant reduction of landfall positional error is noticed in AWiFS data than that of USGS data. The USGS experiments show a south–westward drift of the track just before the landfall process. In case of USGS, the periphery of landfall location is covered with grassland/shrubland/cropland, which significantly cut the moisture resource and with AWiFS data. It is covered with water bodies/evergreen broadleaf forest/irrigated cropland/dryland. Similarly, the north–westward drift in Hudhud cyclone and north–north–eastward drift in Fani cyclone in model simulations with AWiFS datasets are mainly attributed to the roughness contrast and representativeness of AWiFS data. Analysis also shows that for all the land surface parameterization processes except thermal diffusion scheme, the landfall point error is significantly lower with AWiFS experiments. The landfall time error is also substantially reduced in AWiFS experiments for all the cyclones.

The intensity of cyclone in terms of central pressure and maximum sustainable wind illustrates that model

simulation with USGS data has a tendency to intensify the system earlier than observation. Model simulation with AWiFS LULC data gives reasonably good results for the simulation of MSLP and maximum wind, which are closer to the observations.

The spatial distribution of rainfall is analysed for daily accumulated, and model simulated rainfall analysed at the station level too. In case of daily accumulated rainfall, the overestimation of rainfall in USGS experiments is noticed. Also, the USGS experiments provide maximum rainfall over ocean region. In addition to this, the station rainfall clearly suggests that the AWiFS LULC improves the amount of rainfall during the landfall day and reasonably matched with the IMD and GPM observed rainfall for all the cyclones.

The dynamics and the thermodynamic structure of the cyclone Phailin are demonstrated through vorticity and equivalent potential temperature at the landfall day of the storm, and results suggest that both USGS and AWiFS well simulate the structure and vertical extent of the storm.

The overall analysis suggests that the AWiFS LULC with NOAH-MP land surface parameterization scheme in WRF model could well simulate the movement and the intensity of BoB extremely severe cyclonic storm during and after the landfall of the system with reasonable accuracy.

Fig. 7 24-h accumulated rainfall (cm) associated with TC Fani from **a** GPM, **b–e** USGS LULC and **f–i** AWiFS LULC on the landfall day, 03 May 2019

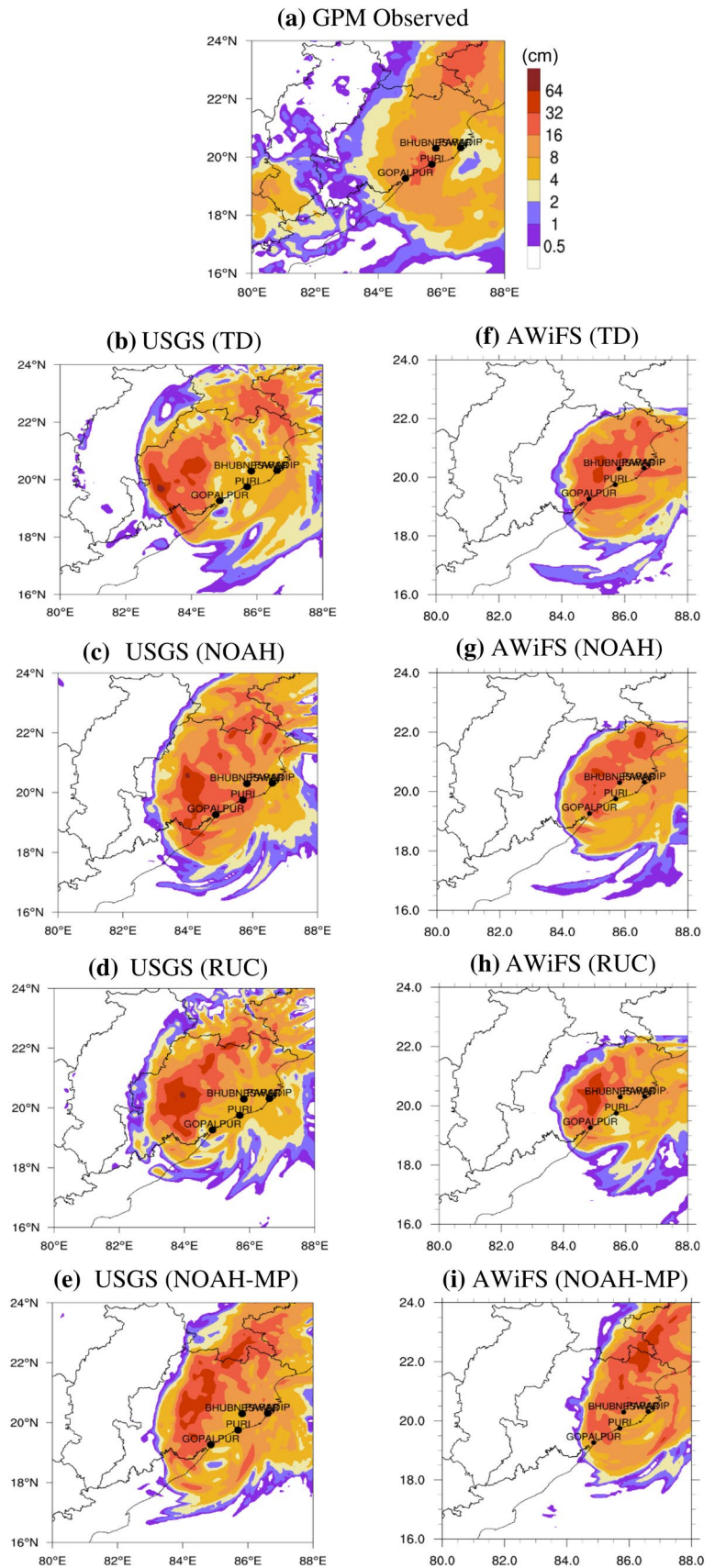


Fig. 8 Comparison of WRF-simulated daily accumulated rainfall associated with TC Fani with IMD and GPM observation over Puri for 01–03 May 2019

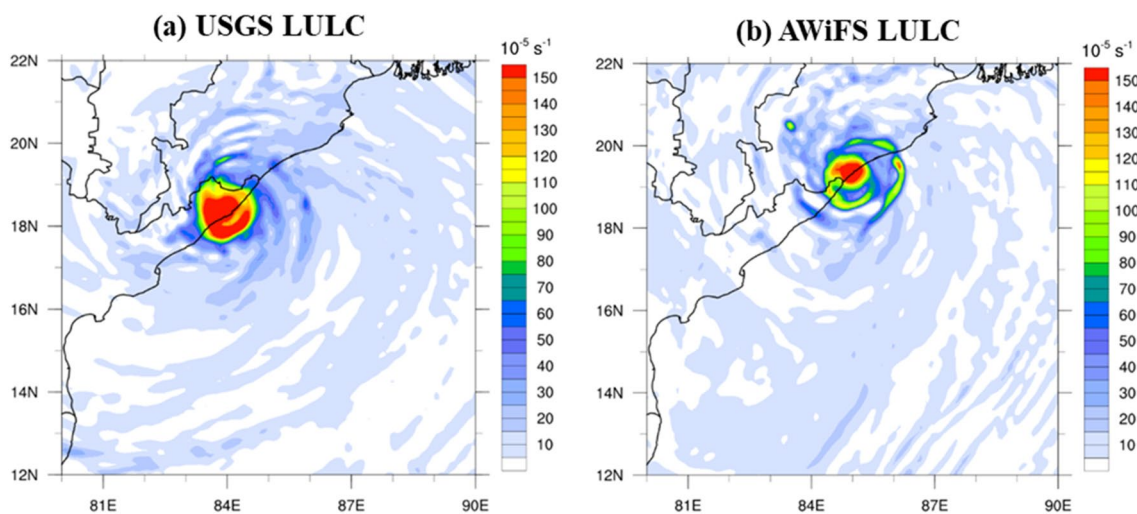
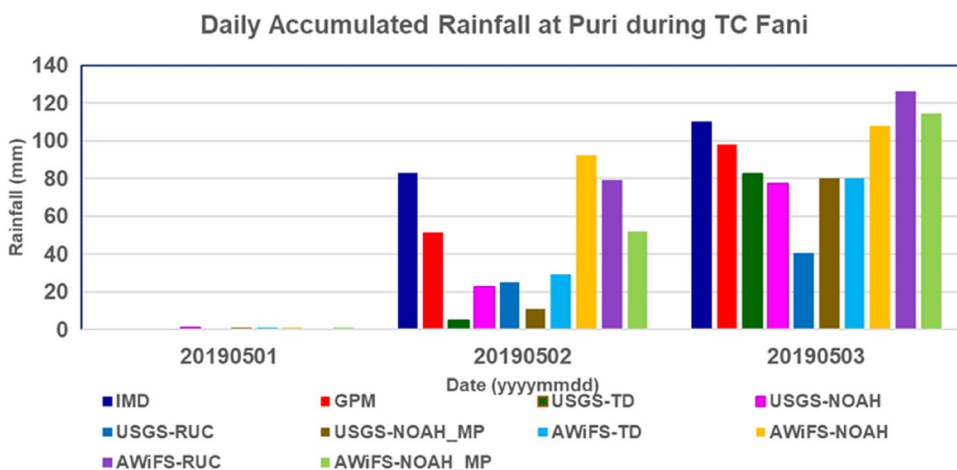


Fig. 9 Spatial distribution of WRF model simulated vorticity at 850 hPa for TC Phailin from **a** USGS LULC, and **b** AWiFS LULC on the landfall day, 12 October 2013

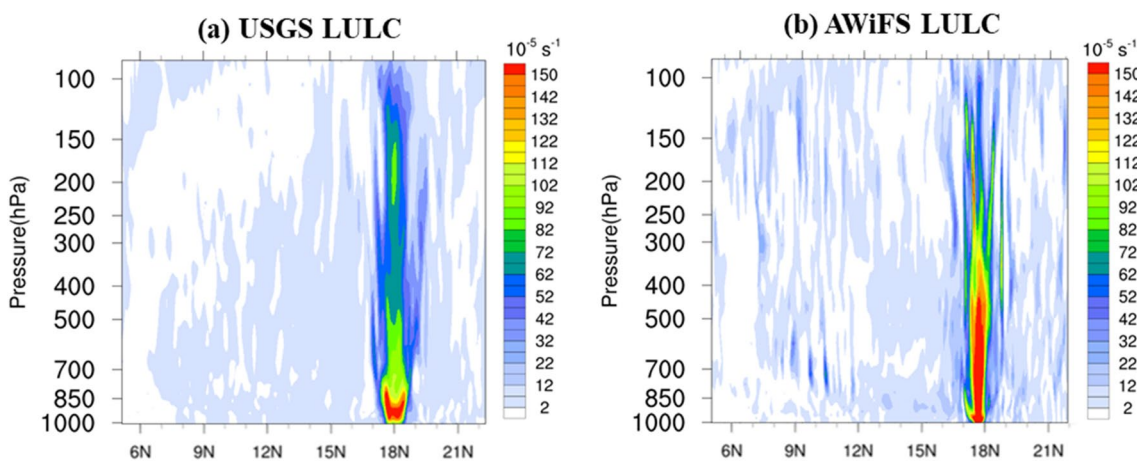


Fig. 10 Latitudinal cross section of vorticity for TC Pailin with **a** USGS LULC and **b** AWiFS LULC on landfall day, 12 October 2013

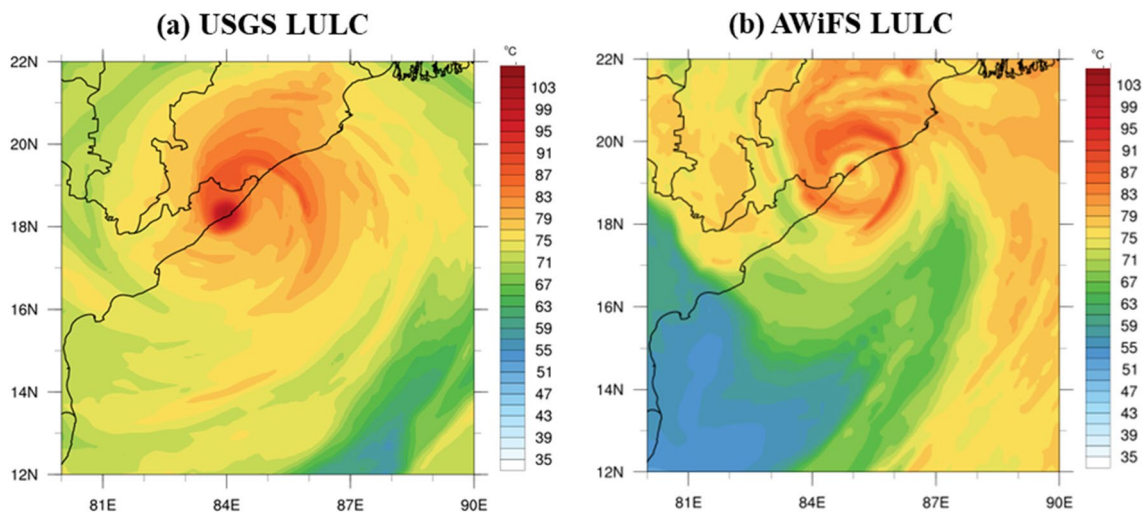


Fig. 11 WRF model simulated equivalent potential temperature at 850 hPa for TC Phailin from **a** USGS LULC, and **b** AWiFS LULC on the landfall day, 12 October 2013

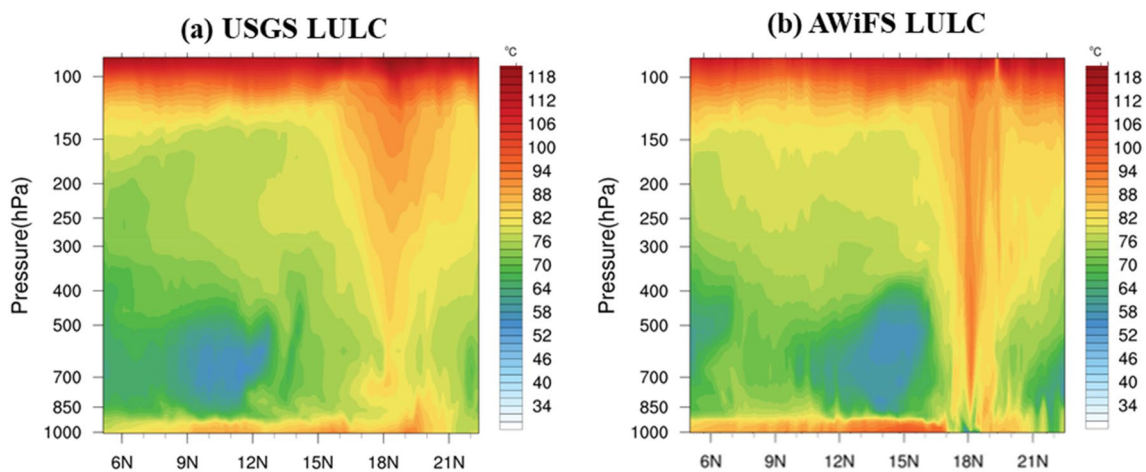


Fig. 12 Vertical cross section of equivalent potential temperature for TC Pailin with **a** USGS LULC and **b** AWiFS LULC on landfall day, 12 October 2023

Acknowledgements The authors sincerely acknowledge the National Oceanic and Atmospheric Administration (NOAA) for providing Global Forecasting System (GFS) initial and boundary data to run WRF model and the National Aeronautics and Space Administration for Global Precipitation Measurement (GPM) rainfall data. The authors are thankful to India Meteorological Department for the observational data and National Remote Sensing Centre (NRSC), ISRO, India for the Land Use/Land Cover data.

Author contributions All authors contributed to the conceptualization of the study. Data acquisition, model run and the first draft of the manuscript were done by PJ. Result analyses were performed by SP and AR. Editing and finalisation of the manuscript by Sushil Kumar and P.V.S. Raju.

Funding The authors declare that there is no financial support received during the preparation of this manuscript.

Data availability The National Centres for Environmental Prediction data (<https://rda.ucar.edu/datasets/ds083.2/>) is utilised for the model's initial and boundary conditions. The USGS (<https://www.usgs.gov/>) provides the USGS-LULC data sets, and the National Remote Sensing Centre (<https://www.nrsc.gov.in/>) provides the AWiFS datasets.

Declarations

Conflict of Interest The authors have no relevant financial or non-financial interests to disclose.

References

- Alapaty K, Niyogi D, Chen F, Pyle P, Chand S, N, (2008) Development of the flux-adjusting surface data assimilation system for mesoscale models. *J of Appl Met and Clim* 47:2331–2350. <https://doi.org/10.1175/2008JAMC1831.1>
- Anantharaj VG, Fitzpatrick PJ, Li Y, King RL, Mostovoy GV (2006) Impact of land use and land cover changes in the surface fluxes of an atmospheric model. In *International Geoscience and Remote Sensing Symposium (IGARSS)* 2369–2372, <https://doi.org/10.1109/IGARSS.2006.613>.
- Anthes RA (1984) Enhancement of convective precipitation by mesoscale variation in vegetative covering in semiarid regions. *J Appl Meteorol* 23:541–554. [https://doi.org/10.1175/1520-0450\(1984\)023<0541:EOCPBM>2.0.CO;2](https://doi.org/10.1175/1520-0450(1984)023<0541:EOCPBM>2.0.CO;2)
- Badarinath KVS, Mahalakshmi DV, Ratna SB (2012) Influence of land use land cover on cyclone track prediction—a study during Aila cyclone. *Open Atmos Sci J* 6:33–41. <https://doi.org/10.2174/1874282301206010033>
- Betts AK, Ball JH, Beljaars ACM, Miller MJ, Viterbo PA (1996) The land surface–atmosphere interaction: a review based on observational and global modeling perspectives. *J Geophys Res* 101(B):7209–7225. <https://doi.org/10.1029/95JD02135>
- Bosart LF, Velden CS, Bracken WE, Molinari J, Black P (2000) Environmental influence on the rapid intensification stage of hurricane Opal (1995) over the Gulf of Mexico. *Mon Weather Rev* 128:322–352. [https://doi.org/10.1175/1520-0493\(2000\)128%3c0322:EIOTRI%3e2.0.CO;2](https://doi.org/10.1175/1520-0493(2000)128%3c0322:EIOTRI%3e2.0.CO;2)
- Chauhan A, Kumar R, Singh RP (2018) Coupling between Land–Ocean–Atmosphere and Pronounced Changes in Atmospheric/Meteorological Parameters Associated with the Hudhud Cyclone of October 2014”. *Int J Environ Res Public Health* 15:2759. <https://doi.org/10.3390/ijerph15122759>
- Collins DC, Avissar R (1994) An evaluation with the Fourier amplitude sensitivity test (FAST) of which land surface parameters are of greatest importance in atmospheric modeling. *J Clim* 7:681–703. [https://doi.org/10.1175/1520-0442\(1994\)007%3c0681:AEWTF%3e2.0.CO;2](https://doi.org/10.1175/1520-0442(1994)007%3c0681:AEWTF%3e2.0.CO;2)
- Gharai B (2014) IRS-P6 AWiFS Derived LU/LC Data Compatible to Mesoscale (WRF) Models Over Indian Region, NRSC Oct 2014, NRSC-ECSA-ACSG-OCT-2014-TR-651
- Gogoi PP, Vinoj V, Swain D, Roberts G, Dash J, Tripathy S (2019) Land use and land cover change effect on surface temperature over Eastern India. *Sci Rep* 9:8859. <https://doi.org/10.1038/s41598-019-45213-z>
- Hong X, Chang SW, Raman S, Shay LK, Hodur R (2000) The interaction between hurricane Opal (1995) and a warm-core ring in the Gulf of Mexico. *Mon Weather Rev* 128:1347–1365. [https://doi.org/10.1175/1520-0493\(2000\)128%3c1347:TIBHOA%3e2.0.CO;2](https://doi.org/10.1175/1520-0493(2000)128%3c1347:TIBHOA%3e2.0.CO;2)
- IMD report (2014) Very severe cyclonic storm, HUDHUD over the Bay of Bengal (07–14 October 2014): A Report, Cyclone Warning Division, India Meteorological Department, New Delhi, pp 66
- IMD report (2019) Extremely severe cyclonic storm, FANI over the Bay of Bengal (26 April–4 May 2019): a Report, Cyclone Warning Division, India Meteorological Department, New Delhi, pp 71
- Johari P, Kumar S, Pattanayak S, Routray A (2022) Performance of land surface schemes on simulation of land falling tropical cyclones over Bay of Bengal using ARW model. *Mausam*. (In Press)
- Karri S, Gharai B, Krishna, SVSS, Rao PVN (2016) Impact of AWiFS derived land use land cover on simulation of heavy rainfall. In: *Proc. SPIE 9882, Remote Sensing and Modeling of the Atmosphere, Oceans, and Interactions VI*, 98821M; <https://doi.org/10.1117/12.2223627>
- Kimball JS (2009) A satellite approach to estimate land-atmosphere CO₂ exchange for boreal and arctic biomes using MODIS and AMSR-E. *IEEE Trans Geol Remote Sens* 47:2. <https://doi.org/10.1109/TGRS.2008.2003248>
- Loveland TR, Reed BC, Brown JF, Ohlen DO, Zhu Z, Yang L, Merchant JW (2020) Development of a global land cover characteristics database and IGBP DISCover from 1 km AVHRR. *Int J Remote Sens* 21(6 & 7):1303–1330. <https://doi.org/10.1080/014311600210191>
- Maxwell RM, Chow FK, Kollet SJ (2007) The groundwater-land surface-atmosphere connection: soil moisture effects on the atmospheric boundary layer in fully-coupled simulations. *Adv Water Resour* 30:2447–2466. <https://doi.org/10.1016/j.advwatres.2007.05.018>
- Mohan M, Kandya A (2015) Impact of urbanization and land-use/land-cover change on diurnal temperature range: A case study of tropical urban airshed of India using remote sensing data. *Sci Total Environ* 506–507:453–465. <https://doi.org/10.1016/j.scitotenv.2014.11.006>
- Mohanty UC, Osuri KK, Routray A, Mohapatra M, Pattanayak S (2010) Simulation of Bay of Bengal tropical cyclones with WRF model: Impact of initial and boundary conditions. *Mar Geodesy* 33:294–314. <https://doi.org/10.1080/01490419.2010.518061>
- Narisma GT, Pitman AJ (2003) The impact of 200 years land cover change on the Australian near-surface climate. *J Hydrometeorol* 4:424–436. [https://doi.org/10.1175/1525-7541\(2003\)4%3c424:TIOYOL%3e2.0.CO;2](https://doi.org/10.1175/1525-7541(2003)4%3c424:TIOYOL%3e2.0.CO;2)
- NRSC (2014) Land Use/Land Cover database on 1:50,000 scale, Natural Resources Census Project, LUCMD, LRUMG, RSAA, National Remote Sensing Centre, ISRO, Hyderabad
- Osuri KK, Mohanty UC, Routray A, Mohapatra M (2012) Real-time track prediction of tropical cyclones over the North Indian Ocean using the ARW model. *J Appl Meteorol Climatol* 52(11):2476–2492. <https://doi.org/10.1175/JAMC-D-12-0313.1>
- Pitman AJ, Narisma GT, Pielke Sr RA, Holbrook NJ (2004) Impact of land cover change on the climate of southwest Western Australia. *J Geophys Res* 109:1–12. <https://doi.org/10.1029/2003JD004347>
- Raju PVS, Potty J, Mohanty UC (2011) Sensitivity of physical parameterizations on prediction of tropical cyclone Nargis over the Bay of Bengal using WRF model. *Meteorol Atmos Phys* 113:125–137. <https://doi.org/10.1007/s00703-011-0151-y>
- Raupach MR (2000) Equilibrium evaporation and the convective boundary layer”. *Bound Layer Meteor* 96:107–141. <https://doi.org/10.1023/A:1002675729075>
- Ravindranath M, Ashrit R (2010) Experiment on utilization of AWiFS LU/LC data in WRF mesoscale model. *NMRF Research Report*, NMRF/RR/01/2010
- Routray A, Mohanty UC, Osuri KK, Kar SC, Niyogi D (2016) Impact of satellite radiance data on simulations of Bay of Bengal tropical cyclones using the WRF-3DVAR modeling system. *IEEE Trans Geosci Remote Sens* 54:2285–2303
- Sateesh M, Srinivas CV, Raju PVS (2017) Numerical simulation of tropical cyclone Thane: role of boundary layer and surface drag parameterization schemes. *Nat Hazards* 89(3):1255–1271. <https://doi.org/10.1007/s11069-017-3020-2>
- Shenoy M, Raju PVS, Prasad VS, Hariprasad KBRR (2022) Sensitivity of physical schemes on simulation of severe cyclones over Bay of Bengal using WRF-ARW model. *Theor Appl Climatol*. <https://doi.org/10.1007/s00704-022-04102-8>
- Singh P, Kikon N, Verma P (2017) Impact of land use change and urbanization on urban heat island in Lucknow city, Central India. A remote sensing based estimate. *Sustain Cities Soc* 32:100–114. <https://doi.org/10.1016/j.scs.2017.02.018>
- Tiwari G, Kumar P (2022) Predictive skill comparative assessment of WRF 4DVar and 3DVar data assimilation: an Indian Ocean tropical cyclone case study. *Atmos Res*. <https://doi.org/10.1016/j.atmosres.2022.106288>
- Tiwari G, Kumar P (2023) Pertaining the application of the 4DVar and 4DVar WRFDA techniques to simulate tropical cyclones in the Bay of Bengal. *Adv Sp Res*. <https://doi.org/10.1016/j.asr.2023.03.015>. (ISSN 0273-1177)
- Wang Y (2002) Vortex Rossby waves in a numerically simulated tropical cyclone. Part II: the role in tropical cyclone structure and intensity

- change. *J Atmos Sci* 59:1239–2126. [https://doi.org/10.1175/1520-0469\(2002\)059%3c1213:VRWIAN%3e2.0.CO;2](https://doi.org/10.1175/1520-0469(2002)059%3c1213:VRWIAN%3e2.0.CO;2)
- Wang B, Elsberry RL, Wang Y, Wu L (1998) Dynamics in tropical cyclone motion: a review. *Chinese J Atmos Sci* 22:535–547
- Wong MLM, Chan JCL (2006) Tropical cyclone motion in response to land surface friction. *J Atmos Sci*. <https://doi.org/10.1175/JAS3683.1>
- Wu C-C, Cheng H-J (1999) An observational study of environmental influences on the intensity changes of typhoons Flo (1990) and Gene (1990). *Mon Wea Rev* 127:3003–3031. [https://doi.org/10.1175/1520-0493\(1999\)127%3c3003:AOSOEI%3e2.0.CO;2](https://doi.org/10.1175/1520-0493(1999)127%3c3003:AOSOEI%3e2.0.CO;2)
- Wu C-C, Emanuel KA (1993) Interaction of a baroclinic vortex with background shear: application to hurricane movement. *J Atmos Sci* 50:62–76. [https://doi.org/10.1175/1520-0469\(1993\)050%3c0062:IOABVW%3e2.0.CO;2](https://doi.org/10.1175/1520-0469(1993)050%3c0062:IOABVW%3e2.0.CO;2)
- Wu C-C, Kurihara Y (1996) A numerical study of the feedback mechanism of hurricane-environment interaction on hurricane movement from the potential vorticity perspective. *J Atmos Sci* 53:2264–2282. [https://doi.org/10.1175/1520-0469\(1996\)053%3c2264:ANSOTF%3e2.0.CO;2](https://doi.org/10.1175/1520-0469(1996)053%3c2264:ANSOTF%3e2.0.CO;2)

Springer Nature or its licensor (e.g. a society or other partner) holds exclusive rights to this article under a publishing agreement with the author(s) or other rightsholder(s); author self-archiving of the accepted manuscript version of this article is solely governed by the terms of such publishing agreement and applicable law.